# Relationship Between the Visual Evoked Potential and Structure in the Primary Visual Cortex in Healthy Individuals and in Patients with Severe Mental Disorders

**Nora Berz Slapø** ( n.b.slapo@medisin.uio.no )
NORMENT, Division of Mental Health and Addiction, Oslo University Hospital and Institute of Clinical Medicine, University of Oslo, Norway

**Kjetil Jørgensen**
NORMENT, Division of Mental Health and Addiction, Oslo University Hospital and Institute of Clinical Medicine, University of Oslo, Norway

**Torbjørn Elvsåshagen**
NORMENT, Division of Mental Health and Addiction, Oslo University Hospital and Institute of Clinical Medicine, University of Oslo, Norway

**Stener Nerland**
NORMENT, Division of Mental Health and Addiction, Oslo University Hospital and Institute of Clinical Medicine, University of Oslo, Norway

**Daniel Roelfs**
NORMENT, Division of Mental Health and Addiction, Oslo University Hospital and Institute of Clinical Medicine, University of Oslo, Norway

**Mathias Valstad**
NORMENT, Division of Mental Health and Addiction, Oslo University Hospital and Institute of Clinical Medicine, University of Oslo, Norway

**Clara Timpe**
NORMENT, Division of Mental Health and Addiction, Oslo University Hospital and Institute of Clinical Medicine, University of Oslo, Norway

**Genevieve Richard**
NORMENT, Division of Mental Health and Addiction, Oslo University Hospital and Institute of Clinical Medicine, University of Oslo, Norway

**Dani Beck**
NORMENT, Division of Mental Health and Addiction, Oslo University Hospital and Institute of Clinical Medicine, University of Oslo, Norway

**Linn Sofie Sæther**
NORMENT, Division of Mental Health and Addiction, Oslo University Hospital and Institute of Clinical Medicine, University of Oslo, Norway

**Maren Werner**
NORMENT, Division of Mental Health and Addiction, Oslo University Hospital and Institute of Clinical Medicine, University of Oslo, Norway
**Trine Lagerberg**
NORMENT, Division of Mental Health and Addiction, Oslo University Hospital and Institute of Clinical Medicine, University of Oslo, Norway
**Ole Andreassen**
NORMENT, Division of Mental Health and Addiction, Oslo University Hospital and Institute of Clinical Medicine, University of Oslo, Norway
**Ingrid Melle**
NORMENT, Division of Mental Health and Addiction, Oslo University Hospital and Institute of Clinical Medicine, University of Oslo, Norway
**Ingrid Agartz**
NORMENT, Division of Mental Health and Addiction, Oslo University Hospital and Institute of Clinical Medicine, University of Oslo, Norway
**Lars T. Westlye**
NORMENT, Division of Mental Health and Addiction, Oslo University Hospital and Institute of Clinical Medicine, University of Oslo, Norway
**Torgeir Moberget**
NORMENT, Division of Mental Health and Addiction, Oslo University Hospital and Institute of Clinical Medicine, University of Oslo, Norway
**Erik G. Jönsson**
NORMENT, Division of Mental Health and Addiction, Oslo University Hospital and Institute of Clinical Medicine, University of Oslo, Norway

---

**Research Article**

**Keywords:** Relationship, visual evoked, primary visual cortex

**Posted Date:** November 10th, 2021

**DOI:** https://doi.org/10.21203/rs.3.rs-990586/v1



---

# Abstract

Schizophrenia (SCZ) spectrum and bipolar disorder (BD) are severe mental disorders with unknown pathophysiology. Altered visual evoked potential (VEP), an electroencephalogram signal reflecting function in the primary visual cortex (V1), abnormal visual processing and visual hallucinations reported in these patients, all point towards V1 dysfunction. While the mechanisms contributing to V1 dysfunction remain unknown, structural alterations are possible candidates. Lack of insight into neural substrates of structure and functional in V1 has limited our ability to determine implications of altered V1 function. While combining VEP and magnetic resonance imaging has increased our understanding of the structure-function relationship in V1 in healthy individuals, no previous study has examined the same structure-function relationship in patients with SCZ spectrum and BD. Here, we aimed to confirm previous findings of a selective positive correlation between the amplitude of the P100 component of the VEP and V1 surface area (SA) in 307 healthy individuals and to examine whether this relationship was altered in patients with SCZ spectrum (n=30) and BD (n=45). The correlation between the P100 amplitude and the total, (r=0.16, p=0.006), right (r=0.14, p=0.013) and left V1 surface area (r=0.13, p=0.02) was significant in healthy individuals, but not in patients. The current results support previous findings of a selective relationship between P100 amplitude and V1 surface area in healthy individuals and suggests that other factors than V1 surface area or thickness explain V1 dysfunction reported in these patients.


# 1. Introduction

Schizophrenia (SCZ) spectrum and bipolar disorders (BD) are severe mental disorders with largely unknown pathophysiology [1–4]. Studies on how the brain processes specific stimuli using electroencephalography (EEG) [5] in the form of event related potential (ERP) techniques have reported abnormal brain function in the primary visual cortex (V1) in these disorders [6–18]. The visual evoked potential (VEP) is a robust ERP signal primarily reflecting post-synaptic potentials of pyramidal cells in V1 and provides information on the functional integrity of the visual system [16,19,20]. In humans, checkerboard reversal stimulation triggers a VEP with three main components, the N75, the P100 and the N145 [5,21], that can be extracted from scalp-recorded EEG. While the exact cortical sources of the VEP components remain to be fully clarified, previous studies suggest that the VEP components are generated mainly in V1 areas [22,23]. See figure 1 illustrating how checkerboard reversal triggers a VEP response that can be recorded with scalp-EEG. The amplitude of the VEP, reflecting function in V1 [20], is reduced in SCZ spectrum disorder [13] and altered VEP plasticity – a correlate of long-term potentiation-like visual cortex plasticity – is described in SCZ spectrum and BD [7,8,14,18]. In addition to altered VEP, abnormal visual processing [24,25], impaired neural activity in V1 areas [26] and visual hallucinations [27–30] all point towards dysfunction in V1 areas in these patients. While the precise mechanisms contributing to such V1 dysfunction remains unknown, structural alterations are possible candidates. While magnetic resonance imaging (MRI) studies show group-level alterations in brain cortical structure [31–42], no studies have reported specific alteration in the V1 surface area or thickness in patients with SCZ spectrum or BD. This suggest that other factors than surface area or thickness in V1 may explain V1 dysfunction, as reflected

by altered VEP in these patients [43–46]. While previous studies have investigated structure and function in the visual cortex with functional MRI (fMRI) [47–50], studies utilized the enhanced spatio-temporal resolution obtained when combining structural MRI (sMRI) and VEP to explore the structure-function relationship in V1 are lacking. While we previously found a positive correlation between the amplitude of the P100 component of the VEP and the V1 surface area [51] in a small sample of healthy individuals, no previous study has examined the same relationship in patients with SCZ spectrum and BD [44,47,48,50]. Combining VEP and sMRI may provide new insights into neural substrates of functional alterations in V1 in these disorders. However, to determine implications of V1 dysfunction in these patients, we first need to gain more knowledge on the structure-function relationship in V1 in healthy individuals. Here, we examined 307 healthy individuals and participants with SCZ spectrum (n=30) or BD (n=30) with a standardized VEP paradigm and brain sMRI with the following main aims: (1) to test the reproducibility of a previously reported positive and selective relationship between the amplitude of the P100 component of the VEP and the V1 surface area in a larger sample of healthy individuals [51], and (2) to assess whether the same structure-function relationship was altered in patients with SCZ spectrum and BD. We hypothesized to find a positive and selective relationship between the P100 amplitude and the surface area, but not thickness of V1 in healthy individuals [51]. Further, we hypothesized to find an altered V1 structure-function relationship in patients with SCZ spectrum and BD. No previous study has shown evidence for reduced V1 surface area or thickness in this patient group. Thus, we hypothesized that other factors than V1 surface area or thickness explain V1 dysfunction as reflected by altered VEP.

# 2. Methods

## 2.1. Sample description

Our study sample included healthy individuals and patients with a diagnosis of SCZ spectrum or BD who participated in the TOP-Study at the Norwegian Centre for Mental Disorders Research (NORMENT) located in Oslo, Norway. Patients with a DSM-IV diagnosis of SCZ spectrum disorder (including schizophrenia, schizophreniform, schizoaffective and psychotic disorder not otherwise specified (NOS)) or BD (including bipolar type 1, bipolar type 2 and bipolar NOS) were included, provided that they were deemed capable of giving formal consent. Healthy individuals were recruited from the national population register in Norway or through advertisement in the local newspaper. Only participants with a normal or corrected-to-normal vision, assessed using a Snellen eye chart, were included. All participants with a history of head trauma with loss of consciousness, an IQ < 70, or a somatic or neurological disorders believed to influence brain function were excluded. Exclusion criteria for healthy individuals were as follows: 1.) any history of mental disorders, severe mental disorders in first degree relatives, 2.) any history of alcohol- and substance abuse or dependence 3.) use of cannabis in the last three months prior to inclusion. Further healthy individuals and patients with any contraindications for MRI (e.g., metallic implants, pacemakers or MRI-incompatible prosthetic heart valves) or EEG examinations (e.g., history of epilepsy), with any incidental findings on the MRI caput indicating brain pathology potentially influence our analyses, with poor quality of V1 area mask and with a time interval between the EEG and

MRI examinations > 11 months were further excluded. In our main and secondary analyses participants with a diagnosis of SCZ spectrum or BD were referred to as patients and analyzed together as one group. An overview of the final study sample is provided in Table 1. The study was approved by the Regional Committees for Medical and Health Research Ethics of South – Eastern Norway. All methods were performed in accordance with the Declaration of Helsinki and the project leader was an authorized clinical psychiatrist, legally obliged to follow the Health Personnel Act. The project was granted with license from Norwegian Information Council (Datatilsynet) to collect and store sensitive information and human biological material until 2050. All participants provided written informed consent. All participation was voluntary and independent of any treatment provided. The participants could whenever they want, withdraw from the study without this having any consequences for the treatment..

Table 1
Demographic table of the final study sample and subgroups separated by diagnosis and sex. All numbers represent the sample after removing outliers as described in 2.3.1. SCZ = schizophrenia. NOS = not otherwise specified. AGE = mean age with age range; sd = standard deviation.

| | sample | females | males | age |
|---|---|---|---|---|
| TOTAL sample | 382 | 231 | 151 | 47 (18 - 85, sd = 17) |
| HEALTHY INDIVIDUALS | 307 | 183 | 124 | 50 (18 – 85, sd = 17) |
| Patients | 75 | 48 | 27 | 33 (18 – 57, sd = 10) |
| SCZ SPECTRUM DISORDERS | 30 | 17 | 13 | 33 (18 – 54, sd = 10) |
| - Schizophrenia | 18 | 7 | 11 | 32 (19 – 54, sd = 10) |
| - Schizoaffective | 3 | 3 | 0 | 32 (28 – 40, sd = 6) |
| - Schizophreniform | 1 | 1 | 0 | 32 (-) |
| - Psychosis nos | 8 | 6 | 2 | 35 (18 – 53, sd = 13) |
| Bipolar disorders | 45 | 31 | 14 | 33 (20 – 57, sd = 11) |
| - Bipolar I | 22 | 17 | 5 | 33 (20 – 57, sd = 11) |
| - Bipolar II | 22 | 13 | 9 | 33 (20 – 53, sd = 11) |
| - Bipolar NOS | 1 | 1 | 0 | 35 (-) |

# 2.2. Data collection and analyses

MRI, EEG data were collected between 2015 and 2019 with a median time interval between MRI and EEG examinations of 17 days (interquartile time difference of 40 days (time difference range 0–321 days)). Clinical examinations were performed during the same time period.

# 2.2.1. MRI acquisition, analyses, quality control and editing

MRI scanning was performed with a General Electric Discovery MR750 3T scanner at the Regional Core Facility for Translational MRI Neuroimaging located at Oslo University Hospital. T1-weighted inversion recovery-prepared 3D gradient recalled echo volumes were acquired using the following parameters: 188 sagittal slices, field of view: 256x256 mm, voxel size: 1x1x1 mm, inversion time: 450 msec, echo time: 3.18 msec, repetition time: 8.16 msec, flip angle: 12°. All MRI scans were processed using FreeSurfer version 6.0 (https://surfer.nmr.mgh.harvard.edu) [52]. In brief, processing steps included removal of non-brain tissue, automatic Talairach transformation and intensity correction. Intensity information was used to reconstruct the inner (i.e., the gray/white matter boundary) and outer (i.e., the gray matter/cerebrospinal fluid boundary) surface of the cerebral cortex through a series of processing steps as previously described [53–55]. Similar to Elvsåshagen et al. (2015) [51], we adopted the methods from Hinds et al. (2008) [55] to obtain measures of the total (right + left), right and left V1 surface area, mean (average) V1 cortical thickness ((right + left V1 cortical thickness) / 2)) in addition to estimated total intracranial volume (eTIV). This method locates the V1 using a surface-based probabilistic atlas derived from high-resolution sMRI of the stria of Gennari. Manual editing of surface reconstruction errors was performed and V1 masks were visually inspected to ensure satisfactory placement. In addition to these quality assurance steps we included FreeSurfer Euler numbers as covariates in our analyses to evaluate MRI image quality [56]. We calculated “the total corrected Euler number” from numbers of holes in the original (non-corrected) cortical surface, using the following formula: 2*(#holes -1) for both the left and right V1 surface area.

## 2.2.2. EEG data acquisition, analyses and quality control

EEG data was collected according to the international 10–20 system from a BioSemi ActiveTwo amplifier. Ag-AgCl scalp electrodes (n=64) recorded brain activity, four external electrodes recorded lateral and vertical movement of the eyes and two external electrodes recorded the heart rhythm (electrocardiography). Potentials at each channel were sampled at 2048 Hz with respect to a common mode sense with a driven right leg electrode minimizing common mode voltages. The VEP paradigm was adopted from Normann et al. [57]. In the current study we focused on VEPs elicited during a prolonged period of pattern reversing checkerboards, where checkerboards changed color from white to black with a spatial frequency of 1 cycle/degree over ~ 28 ° visual angle and a fixed frequency of 2 reversals per second. We extracted N75, P100 and N145 amplitudes from the intervention phase of the VEP paradigm that lasted 10 min, yielding a total of 1200 reversals. After collecting offline VEPs, the EEG data was processed as described previously [18,58,59] using MATLAB and the EEGLAB toolbox for MATLAB [60]. After down-sampling to 512 Hz, noisy channels were interpolated using the Prep-Pipeline algorithms [61] with default mode while muscle, eye blinks and eye movement artefacts were eliminated using SASICA defaults [62]. We decomposed the EEG data into independent components using the SOBI algorithm [63]. Epochs with amplitude exceeding 100 μV were removed and the AFz electrode was used as the reference electrode for all channels. ERPs were extracted from the Oz channel. As a quality index for EEG, we computed the standard error (across trials) of the VEP amplitudes for each participant, and standardized

this index by dividing them by the mean VEP amplitudes (i.e., expressing the cross-trial variance as a percentage of the total amplitude). See figure 1 illustrating the VEP experiment.

# 2.3. Statistical analyses

All statistical analyses were conducted in R version 3.6. (https://www.r-project.org, R Core Team, 2014) and figures were produced using the ggplot2 package implemented in R (Wickham, 2009). For the primary analyses we corrected for multiple testing by dividing p=0.05 by the number of independent analyses performed in this section (n=3), yielding a corrected p-value of <0.02. For our secondary analyses a corrected p-value of <0.008 (p=0.05 / 6) was considered significant. The vertex wise analyses were corrected for multiple testing separately.

# 2.3.1. Outlier removal, tests of data distribution and testing for potential effects of covariates

Outliers were removed using the Routliers package implemented in R studio, which uses a 3.5 median absolute deviation as threshold. Participant were removed based on deviating total V1 surface area, V1 cortical thickness, P100 amplitude, eTIV, Euler numbers or standard error for P100 amplitude. The one-sampled Kolmogorov-Smirnov test revealed normal distribution of the total V1 surface area and V1 cortical thickness in healthy controls and in patients, while the P100 amplitude was normally distributed in patients but not in healthy individuals. We decided to use the Pearson correlation test due to a large sample size, but also ran Kendall and Spearman test to ensure that the choice of correlation test did not influence the results (see supplementary analyses 1.4. for more detail). To test for potential effects of covariates (age, sex, diagnosis, eTIV, Euler number, standard error for P100 amplitude) on our structural (V1 surface area or thickness) and functional (VEP amplitude) outcome measures, we ran linear models and corrected for effects of predictors prior to running correlation analyses between V1 structure and function. In our group of healthy individuals eTIV (t=7.15, p=6.79e-12) and linear age (t=-5.50, p=8.16e-08) showed significant effects on total V1 surface area, while sex (male) showed significant effect on the P100 amplitude (t=-3.64, p=0.0003), and age (cubic age: t=2.51, p=0.013, linear age: t=-8.23, p=5.8e-15) significantly influenced V1 cortical thickness. In our patient group, eTIV (t=5.22 p=1.87e-06), age (linear age: t=2.31, p=0.024) and Euler number (t=-3.02, p=0.04) had significant effects on total V1 surface area, while no other covariates influenced P100 amplitude or V1 cortical thickness significantly.

# 2.3.2. Primary analyses

# 2.3.2.1. Correlation between the P100 amplitude and V1 surface in healthy individuals and in patients

To replicate previous findings of an intimate relationship between V1 structure and function in healthy individuals, we ran partial Pearson correlation analyses between the P100 amplitude and the total, the right and the left V1 surface area. Prior to running correlation analyses we corrected for the effect of age, sex, eTIV and Euler number on V1 surface area, and for effects of age, sex and standard error for P100

amplitude on the P100 amplitude, in healthy individuals (n= 307). To test our hypothesis that the same structure-function relationship was altered in patients with SCZ spectrum and BD, we ran the same correlation analyses in our patient group and performed the paired r test implemented in R to assess whether the P100-V1 correlation was significantly different between healthy individuals and patients.

## 2.3.3. Secondary analyses

### 2.3.3.1. Correlation between P100 amplitude and V1 cortical thickness in healthy individuals and patients

As part of our secondary analyses, we ran correlation analyses between P100 amplitude (corrected for effects of age, sex and standard error for P100 amplitude) and V1 cortical thickness (corrected for effects of age, sex, eTIV and Euler number) in healthy individuals (n=307) and in patients (n=75).

### 2.3.3.2 Correlation between the amplitude of the other VEP components and V1 structure (surface area and cortical thickness) in healthy individuals

To test whether the relationship between V1 surface area and VEP amplitude was specific to the P100 component of the VEP, we ran correlation analyses between the amplitude of N75 and N145, and V1 surface area and V1 cortical thickness in our group of healthy individuals (n=307). Prior to running analyses, we corrected the effects of the same covariates on V1 surface area as mentioned in 2.3.2.1, for effects of the same covariates on V1 cortical thickness as mentioned in 2.3.3.1. and for the effects of age, sex and standard error for N75 on the N75 amplitude and for effect of age, sex and standard error for N145 on the N145 amplitude.

### 2.3.3.3. Vertex- wise whole brain analyses in healthy individuals

To test if a putative relationship between the P100 amplitude was specific to the surface area in V1, we ran whole cortex analyses in our group of healthy individuals. General linear models (GLMs), implemented in FreeSurfer 6.0 were used to test the associations between P100 amplitude and surface area in each vertex of the cortical surface, correcting for the effects of age, sex, eTIV and Euler number. A different offset, same slope model was specified. Similar models were used to test all associations specified above. To correct for multiple testing across space, cluster-wise correction was performed using the following parameters: Cluster-forming threshold: $p<0.05$, unsigned; precomputed Monte Carlo simulation (–cache); cluster-wise probability: $p<0.05$; correction for analyses of two hemispheres (--2spaces) applied.

## 3. Results

# 3.1. Primary results

## 3.1.1. Correlation between the P100 amplitude and V1 surface in healthy individuals and in patients

We found a positive correlation between the P100 amplitude and the total, the right and the left V1 surface area in healthy individuals (n=307), but not in patient (n=75). The paired r test revealed that the correlation between P100 and V1 surface area was not significantly different in healthy individuals compared to patients. See figure 2 illustrating the results. A corrected p-value of <0.02 was considered significant.

# 3.2. Secondary results

## 3.2.1.1. Correlation between P100 amplitude and V1 cortical thickness in healthy individuals and patients

We did not find any significant correlation between the P100 amplitude and V1 cortical thickness in healthy individuals (n=307) or in patients. A corrected p-value of <0.008 was considered significant. See figure 3 illustrating the result.

## 3.2.1.2 Correlation between the amplitude of the other VEP components and V1 structure (surface area and cortical thickness) in healthy individuals

We did not find any significant correlation between the amplitude of the N75 and the total (r=-0.007, p=0.9), the right (r=0.02, p=0.73) or the left (r=-0.033, p=0.57) V1 surface area or V1 cortical thickness (r=-0.0002, p=1). Further, we observed no significant correlation between the N145 and the total (r=-0.085, p=0.14), the right (r=-0.042, p=0.47) or the left (r=-0.11, p=0.062) V1 surface area or V1 cortical thickness (r=-0.098, p=0.087). A corrected p-value of <0.008 was considered significant.

## 3.2.2. Vertex-wise whole brain analyses in healthy individuals

Before correction for multiple testing, we observed a bilateral positive association between the P100 amplitude and V1 surface area (p< 0.01, uncorrected). No other cortical regions were observed to have similar correlations in both hemispheres. However, after cluster-wise correction for multiple testing, findings of a positive association in the V1 were no longer significant. See figure 4 illustrating significant correlation between P100 amplitude and surface area in each hemisphere.

# 4. Discussion

The current study confirms our hypothesis and previous findings of an intimate relationship between V1 surface area, but not thickness, and V1 function, reflected by P100 amplitude, in healthy individuals [51]. The non-significant correlation between P100 amplitude and V1 structure (surface area and thickness) in our patient group, support our hypothesis of an altered structure-function relationship in SCZ spectrum and BD.

## 4.1. Underlying mechanism explaining the correlation between surface area and function in V1 in healthy individuals

The exact mechanism explaining the positive correlation between V1 surface area and function in the same area, as reflected by P100 amplitude in healthy individuals remains elusive. However, the pool of synapses and the width and/or the number of cortical columns in V1 potentially increases with enlarged surface area, enhancing the summation of postsynaptic potentials (PSP) generated by V1 pyramidal neurons. Since the P100 amplitude primary reflects PSP in V1 pyramidal cells, a greater summation of PSP with a larger surface area may explain the positive correlation between V1 surface area and the P100 amplitude [44]. Further, the level axonal myelination in V1 may correlate with the V1 surface area in healthy individuals. Enhanced axonal myelination with larger V1 surface area may enable V1 neurons to fire more synchronously [45,49,64–67]. Since scalp EEG reflect only synchronized neuronal activity, a larger surface area and enhanced myelination in V1 may result in a larger P100 amplitude. Further, the level of myelination influences the conduction velocity of action potentials (AP) through presynaptic axons. If APs from a large group of presynaptic cells arrive at the presynaptic terminal simultaneously, neurotransmitters are released from the presynaptic cell into the synaptic cleft, bind to the receptors on the postsynaptic pyramidal neurons and generate PSPs. The summation of a PSPs from large groups of synchronized neurons can be recorded with scalp electrodes (EEG) with a larger P100 amplitude reflecting enhanced summation of PSPs. Since the V1 is highly myelinated, the level of myelination in V1 may mirror function in the same area as reflected by P100 amplitude, either by enhancing summation of PSPs or indirectly by increasing the diameter of pyramidal axons, or both [64,65,67–70]. Precisely how the level of myelination in V1 mirrors P100 amplitude remains elusive, but are research topics we plan to study in the future. Further, the level of neurotransmitters released by presynaptic neurons, either in the form of glutamate or gamma aminobutyric acid (GABA) possibly indirectly affects generation of PSPs in pyramidal cells [71,72]. A larger number of synapses may correlate with an increased release of excitatory neurotransmitters (glutamate) and enhanced summation of PSPs, further explaining our findings of a positive relationship between P100 amplitude and V1 surface area. However, while we know that the level of GABA and glutamate influences the activation of neurons, exactly how these neurotransmitter influence VEP amplitudes, remains elusive.

## 4.2. The structure-function relationship in V1 in patients with SCZ spectrum and BD

While reduced P100 amplitude and V1 dysfunction has been reported in patients with SCZ spectrum and BD, no previous study has demonstrated altered V1 surface area or thickness in these patients, suggesting that other factors than altered V1 surface area or thickness explain V1 dysfunction. Of interest, in the current study we found no significant difference in mean total V1 surface area or mean P100 amplitude between patients and healthy individuals (see Supp Fig. 7 in supplementary information). However, to our knowledge, no previous study has combined sMRI and VEP to investigated whether and how V1 structure mirrors V1 function in patients with SCZ spectrum and BD. While the P100-V1 correlation was not significantly different between healthy individuals and patients, the current and previous findings support our hypothesis that other factor than reduced V1 surface area explains reduced VEP amplitude [13] and altered VEP plasticity [7,8,14,18] in these patients. To this end, we can only speculate about what factors might explain V1 dysfunction that manifested clinically as visual hallucinations [27–30] and altered visual processing [24,25]. While patients with SCZ spectrum show reduced number and degeneration of V1 neurons in addition to reduced V1 volume, whether and how these factors correlate with V1 function, as reflected by VEP, remains unknown [46,73,74]. Synaptic dysfunction [75], aberrant synchronization [76,77], abnormal regulation of neurotransmitters [72,78] and /or abnormal myelination in V1 [79–83] may also explain altered function in V1 in these patients. Further, diminished dendritic arborization of V1 neurons and altered synaptic pruning in SCZ spectrum disorders may result in reduced summation of PSPs and hence reduced P100 amplitude. Since the process of synaptic pruning is preceded by the development of the V1 cortex (including V1 surface area and thickness) abnormal synaptic pruning could explain altered VEP with normal V1 surface area and V1 cortical thickness in patients with SCZ spectrum and BD [84–86]. Studies examining the exact mechanisms to which all factors mentioned above might influence VEP characteristics are missing. Knowledge on how these (structural) factors influence function in V1 may provide new insight into the neural substrates of altered brain function in severe mental disorders. While previous studies show evidence for altered myelination in the visual cortex in patients with SCZ spectrum and BD [79–83], whether and how altered myelination explains V1 dysfunction, remains unknow. Combining MRI measures of myelination and VEP measures reflecting function in V1 may reveal whether abnormal myelination in V1 can explain V1 dysfunction, exhibited clinically as visual hallucinations and altered visual processing.

## 4.3. Why is V1 surface area, but not V1 cortical thickness associated with the P100 amplitude?

Current and previous evidence for a correlation between the P100 amplitude and the surface area, but not the thickness of V1 in healthy individuals indicate that surface area and thickness influence cortical function in different ways. Cortical surface area and thickness are both heritable traits, but differ phenotypically and genetically and result from different ontogenetic stages during development of the cortex [38,87–95]. While cortical thickness is considered to be influenced by environmental and neurodegenerative factors, cortical surface area appears more determined by genetics and is influenced by early neurodevelopmental factors [38,88,92–94,96]. Further, cortical surface area is determined by the total number of cortical columns while cortical thickness is influenced by the number of cells within each

cortical column [90,91]. The selective relationship between P100 amplitude and the surface area, but not thickness in V1 might be due to the organization of the cortex in columns and lamina, where the number and/or width of vertical columns correlated positively with surface area, but not thickness in V1 [91]. Schwarzkopf and colleagues argued that their findings of a selective relationship between cortical surface area, but not thickness and the gamma-band frequency EEG signal was unrelated to gray matter volume, and that the distance across the cortical sheet was the relevant factor for the association [44]. Although speculative, increased surface area may reflect an increased number of vertically organized pyramidal cells in V1 while an increase in cortical thickness may mirrors increased length of pyramidal axons, which does not result in enhanced PSPs reflected by increased P100 amplitude. Intriguingly, one of few previous ERP-MRI studies revealed a significant, but negative correlation between the auditory N1 amplitude, an ERP component reflecting function in the auditory cortex, and the thickness, but not surface area, in the auditory cortex. These findings support previous reports a positive correlation between thinner cortex and function in the auditory cortex [97,98]. Albeit findings of a positive correlation between N1 amplitude and thickness in the auditory cortex is not directly comparable to the current study findings, these results may suggest that increased surface area and thinner cortex mirror increased neural activity in some cortical brain areas [99].

## 4.4. Strengths and limitations

Compared to the previous study by Elvsåshagen and colleagues [51], we corrected for the effect of additional potential confounders on our MRI and ERP measures prior to running analyses. Further, we performed extensive quality control on our structural and functional measures, including adding Euler numbers as a quality index for MRI and standard error for P100 amplitude to control for poor EEG quality. Lack of power due to a limited number of patients included complicated the interpretation of our results. Further, we were not able to control for potential effects of skull thickness, cerebrospinal fluid and meninges on the conductance of electromagnetic fields from their neural sources to scalp electrodes. This should preferably be accounted for when analyzing ERP data. Further, we did not correct for plausible effects of medication use, disease states or symptom severity, including prevalence of visual hallucinations for the patients included.

# 5. Conclusion

The current study findings support the hypothesis of an intimate relationship between the surface area and function in V1 in healthy individuals and shows evidence for an altered structure-function relationship in patients with SCZ spectrum and BD. We need to investigating the relationship between V1 function, as reflected by VEP, and structural components in V1 other than surface area and thickness to gain new insight into neural substrates of altered V1 function in these patients.

# Declarations

### Acknowledgements

Research Council of Norway (223273, 274359, 249795, 248238), the South – Eastern Norway Regional Health Authority (2014097, 2015044, 2015073, 2017097, 2018037, 2018076), the Norwegian Extra Foundation for Health and Rehabilitation (2015/FO5146), the European Research Council under the European Union's Horizon 2020 research and Innovation program (ERC StG 802998), the Ebbe Frøland foundation and a research grant from Mrs. Throne-Holst funded this study. T.E. received speaker's honoraria from Lundbeck and Janssen Cilag and is a consultant to BrainWaveBank. O.A.A. has received speaker's honorarium from Lundbeck and Sunovion and is a consultant to HealthLytix. The other authors report no conflicts of interest. EEG data is currently not openly available due to ethical and privacy issues of clinical data. All codes used for the statistical analyses are available through R studio.

## Author contribution

Nora Berz Slapø: conceptualization, methodology, formal analysis, investigation, visualization and writing original draft.

Kjetil Nordbø Jørgensen: conceptualization, methodology, MRI data acquisition, editing and visualization, supervision, review and editing of manuscript

Torbjørn Elvsåshagen: EEG data acquisition, conceptualization, methodology, supervision, review and editing of manuscript

Torgeir Moberget: conceptualization, methodology, review and editing of manuscript and supervision

Stener Nerland: MRI data acquisition, editing and visualization, review and editing of manuscript

Daniel Roelfs: EEG data acquisition, visualization, review and editing of manuscript

Mathias Valstad: EEG data acquisition, processing, editing and visualization of EEG data, review and editing of manuscript

Clara M. F. Timpe: EEG data acquisition, review and editing of manuscript

Geneviève Richard: MRI data acquisition, EEG data acquisition

Dani Beck: MRI data acquisition, EEG data acquisition, review and editing of manuscript

Linn Sofie Sæther: EEG data acquisition, review and editing of manuscript

Maren C. Frogner Werner: Clinical inclusion, review and editing of manuscript

Trine Vik Lagerberg: Project administration, review and editing of manuscript

Ingrid Melle: Project administration, review and editing of manuscript

Ingrid Agartz: Project administration, review and editing of manuscript

Lars T. Westlye: Project administration, review and editing of manuscript

Ole A. Andreassen: conceptualization and project administration, review and editing of manuscript

Erik G. Jönsson: project administration, conceptualization, methodology, review and editing of manuscript and supervision

### Conflicts of interest

The authors have no conflict of interest to report.

### Data availability

MRI and EEG data used in the following study is currently not openly available due to ethical and privacy issues of clinical data.

## References


1. Birur, B., Kraguljac, N. V., Shelton, R. C. & Lahti, A. C. Brain structure, function, and neurochemistry in schizophrenia and bipolar disorder-a systematic review of the magnetic resonance neuroimaging literature. *NPJ Schizophr* **3**, 15, doi:10.1038/s41537-017-0013-9 (2017).
2. Grande, I., Berk, M., Birmaher, B. & Vieta, E. Bipolar disorder. *Lancet* **387**, 1561-1572, doi:10.1016/S0140-6736(15)00241-X (2016).
3. McGrath, J., Saha, S., Chant, D. & Welham, J. Schizophrenia: a concise overview of incidence, prevalence, and mortality. *Epidemiol Rev* **30**, 67-76, doi:10.1093/epirev/mxn001 (2008).
4. Merikangas, K. R. *et al.* Prevalence and Correlates of Bipolar Spectrum Disorder in the World Mental Health Survey InitiativeBipolar Spectrum in World Mental Health Survey. *JAMA Psychiatry* **68**, 241-251, doi:10.1001/archgenpsychiatry.2011.12 (2011).
5. Luck, S. J. *An introduction to the event-related potential technique*. Second edition. edn, (The MIT Press, 2014).
6. Balz, J. *et al.* Beta/Gamma Oscillations and Event-Related Potentials Indicate Aberrant Multisensory Processing in Schizophrenia. *Frontiers in Psychology* **7**, doi:10.3389/fpsyg.2016.01896 (2016).
7. Cavus, I. *et al.* Impaired visual cortical plasticity in schizophrenia. *Biol Psychiatry* **71**, 512-520, doi:10.1016/j.biopsych.2012.01.013 (2012).
8. Elvsashagen, T. *et al.* Evidence for impaired neocortical synaptic plasticity in bipolar II disorder. *Biol Psychiatry* **71**, 68-74, doi:10.1016/j.biopsych.2011.09.026 (2012).
9. Haigh, S. M., Coffman, B. A., Murphy, T. K., Butera, C. D. & Salisbury, D. F. Abnormal auditory pattern perception in schizophrenia. *Schizophr Res* **176**, 473-479, doi:10.1016/j.schres.2016.07.007 (2016).
10. Javitt, D. C. & Freedman, R. Sensory processing dysfunction in the personal experience and neuronal machinery of schizophrenia. *Am J Psychiatry* **172**, 17-31, doi:10.1176/appi.ajp.2014.13121691 (2015).

11. Pfefferbaum, A., Roth, W. T. & Ford, J. M. Event-related potentials in the study of psychiatric disorders. *Arch Gen Psychiatry* **52**, 559-563, doi:10.1001/archpsyc.1995.03950190041006 (1995).
12. Rosburg, T., Boutros, N. N. & Ford, J. M. Reduced auditory evoked potential component N100 in schizophrenia–a critical review. *Psychiatry Res* **161**, 259-274, doi:10.1016/j.psychres.2008.03.017 (2008).
13. Yeap, S. *et al.* Visual sensory processing deficits in Schizophrenia and their relationship to disease state. *Eur Arch Psychiatry Clin Neurosci* **258**, 305-316, doi:10.1007/s00406-008-0802-2 (2008).
14. Zak, N. *et al.* Longitudinal and cross-sectional investigations of long-term potentiation-like cortical plasticity in bipolar disorder type II and healthy individuals. *Translational Psychiatry* **8**, 103, doi:10.1038/s41398-018-0151-5 (2018).
15. Halliday, A. M., McDonald, W. I. & Mushin, J. Visual evoked response in diagnosis of multiple sclerosis. *Br Med J* **4**, 661-664, doi:10.1136/bmj.4.5893.661 (1973).
16. Tobimatsu, S. & Celesia, G. G. Studies of human visual pathophysiology with visual evoked potentials. *Clin Neurophysiol* **117**, 1414-1433, doi:10.1016/j.clinph.2006.01.004 (2006).
17. Normann, C., Schmitz, D., Fürmaier, A., Döing, C. & Bach, M. Long-Term Plasticity of Visually Evoked Potentials in Humans is Altered in Major Depression. *Biological Psychiatry* **62**, 373-380, doi:https://doi.org/10.1016/j.biopsych.2006.10.006 (2007).
18. Valstad, M. *et al.* Evidence for Reduced Long-Term Potentiation-Like Visual Cortical Plasticity in Schizophrenia and Bipolar Disorder. *Schizophr Bull*, doi:10.1093/schbul/sbab049 (2021).
19. Creel, D. J. Visually evoked potentials. *Handb Clin Neurol* **160**, 501-522, doi:10.1016/B978-0-444-64032-1.00034-5 (2019).
20. Hamilton, R. *et al.* VEP estimation of visual acuity: a systematic review. *Doc Ophthalmol*, doi:10.1007/s10633-020-09770-3 (2020).
21. Sarnthein, J., Andersson, M., Zimmermann, M. B. & Zumsteg, D. High test-retest reliability of checkerboard reversal visual evoked potentials (VEP) over 8 months. *Clin Neurophysiol* **120**, 1835-1840, doi:10.1016/j.clinph.2009.08.014 (2009).
22. Di Russo, F. *et al.* Identification of the neural sources of the pattern-reversal VEP. *Neuroimage* **24**, 874-886, doi:https://doi.org/10.1016/j.neuroimage.2004.09.029 (2005).
23. Vanni, S. *et al.* Sequence of pattern onset responses in the human visual areas: an fMRI constrained VEP source analysis. *Neuroimage* **21**, 801-817, doi:10.1016/j.neuroimage.2003.10.047 (2004).
24. Butler, P. D. *et al.* Subcortical visual dysfunction in schizophrenia drives secondary cortical impairments. *Brain* **130**, 417-430, doi:10.1093/brain/awl233 (2007).
25. Butler, P. D. *et al.* Dysfunction of early-stage visual processing in schizophrenia. *Am J Psychiatry* **158**, 1126-1133, doi:10.1176/appi.ajp.158.7.1126 (2001).
26. Chen, X. *et al.* Irreversible Primary Visual Cortex Impairment in a Mouse Model of High-Risk Schizophrenia. *Neuropsychiatr Dis Treat* **17**, 277-282, doi:10.2147/NDT.S246163 (2021).

27. Waters, F. *et al.* Visual hallucinations in the psychosis spectrum and comparative information from neurodegenerative disorders and eye disease. *Schizophr Bull* **40 Suppl 4**, S233-245, doi:10.1093/schbul/sbu036 (2014).
28. Baethge, C. *et al.* Hallucinations in bipolar disorder: characteristics and comparison to unipolar depression and schizophrenia. *Bipolar Disorders* **7**, 136-145, doi:https://doi.org/10.1111/j.1399-5618.2004.00175.x (2005).
29. Ford, J. M. *et al.* Visual hallucinations are associated with hyperconnectivity between the amygdala and visual cortex in people with a diagnosis of schizophrenia. *Schizophr Bull* **41**, 223-232, doi:10.1093/schbul/sbu031 (2015).
30. Klein, S. D., Olman, C. A. & Sponheim, S. R. Perceptual Mechanisms of Visual Hallucinations and Illusions in Psychosis. *J Psychiatr Brain Sci* **5**, doi:10.20900/jpbs.20200020 (2020).
31. Hallahan, B. *et al.* Structural magnetic resonance imaging in bipolar disorder: an international collaborative mega-analysis of individual adult patient data. *Biol Psychiatry* **69**, 326-335, doi:10.1016/j.biopsych.2010.08.029 (2011).
32. Hartberg, C. B. *et al.* Brain cortical thickness and surface area correlates of neurocognitive performance in patients with schizophrenia, bipolar disorder, and healthy adults. *J Int Neuropsychol Soc* **17**, 1080-1093, doi:10.1017/S1355617711001081 (2011).
33. Lim, C. S. *et al.* Longitudinal neuroimaging and neuropsychological changes in bipolar disorder patients: review of the evidence. *Neurosci Biobehav Rev* **37**, 418-435, doi:10.1016/j.neubiorev.2013.01.003 (2013).
34. Lyoo, I. K. *et al.* Regional cerebral cortical thinning in bipolar disorder. *Bipolar Disord* **8**, 65-74, doi:10.1111/j.1399-5618.2006.00284.x (2006).
35. Madre, M. *et al.* Structural abnormality in schizophrenia versus bipolar disorder: A whole brain cortical thickness, surface area, volume and gyrification analyses. *NeuroImage. Clinical* **25**, 102131-102131, doi:10.1016/j.nicl.2019.102131 (2020).
36. Minuzzi, L. *et al.* Structural and functional changes in the somatosensory cortex in euthymic females with bipolar disorder. *Aust N Z J Psychiatry* **52**, 1075-1083, doi:10.1177/0004867417746001 (2018).
37. Rimol, L. M. *et al.* Cortical thickness and subcortical volumes in schizophrenia and bipolar disorder. *Biol Psychiatry* **68**, 41-50, doi:10.1016/j.biopsych.2010.03.036 (2010).
38. Rimol, L. M. *et al.* Cortical Volume, Surface Area, and Thickness in Schizophrenia and Bipolar Disorder. *Biological Psychiatry* **71**, 552-560, doi:https://doi.org/10.1016/j.biopsych.2011.11.026 (2012).
39. Kuperberg, G. R. *et al.* Regionally localized thinning of the cerebral cortex in schizophrenia. *Arch Gen Psychiatry* **60**, 878-888, doi:10.1001/archpsyc.60.9.878 (2003).
40. van Erp, T. G. M. *et al.* Cortical Brain Abnormalities in 4474 Individuals With Schizophrenia and 5098 Control Subjects via the Enhancing Neuro Imaging Genetics Through Meta Analysis (ENIGMA) Consortium. *Biol Psychiatry* **84**, 644-654, doi:10.1016/j.biopsych.2018.04.023 (2018).

41. Dietsche, B., Kircher, T. & Falkenberg, I. Structural brain changes in schizophrenia at different stages of the illness: A selective review of longitudinal magnetic resonance imaging studies. *Aust N Z J Psychiatry* **51**, 500-508, doi:10.1177/0004867417699473 (2017).
42. Morch-Johnsen, L. *et al.* Auditory Cortex Characteristics in Schizophrenia: Associations With Auditory Hallucinations. *Schizophr Bull* **43**, 75-83, doi:10.1093/schbul/sbw130 (2017).
43. Yoon, J. H. *et al.* GABA concentration is reduced in visual cortex in schizophrenia and correlates with orientation-specific surround suppression. *J Neurosci* **30**, 3777-3781, doi:10.1523/JNEUROSCI.6158-09.2010 (2010).
44. Schwarzkopf, D. S., Robertson, D. J., Song, C., Barnes, G. R. & Rees, G. The frequency of visually induced γ-band oscillations depends on the size of early human visual cortex. *The Journal of neuroscience : the official journal of the Society for Neuroscience* **32**, 1507-1512, doi:10.1523/JNEUROSCI.4771-11.2012 (2012).
45. Engel, A. K., König, P., Kreiter, A. K. & Singer, W. Interhemispheric synchronization of oscillatory neuronal responses in cat visual cortex. *Science* **252**, 1177-1179, doi:10.1126/science.252.5009.1177 (1991).
46. Dorph-Petersen, K. A., Pierri, J. N., Wu, Q., Sampson, A. R. & Lewis, D. A. Primary visual cortex volume and total neuron number are reduced in schizophrenia. *J Comp Neurol* **501**, 290-301, doi:10.1002/cne.21243 (2007).
47. Genc, E., Bergmann, J., Singer, W. & Kohler, A. Surface area of early visual cortex predicts individual speed of traveling waves during binocular rivalry. *Cereb Cortex* **25**, 1499-1508, doi:10.1093/cercor/bht342 (2015).
48. Lee, W. C. *et al.* Anatomy and function of an excitatory network in the visual cortex. *Nature* **532**, 370-374, doi:10.1038/nature17192 (2016).
49. Schwarzkopf, D. S., Robertson, D. J., Song, C., Barnes, G. R. & Rees, G. The frequency of visually induced gamma-band oscillations depends on the size of early human visual cortex. *J Neurosci* **32**, 1507-1512, doi:10.1523/JNEUROSCI.4771-11.2012 (2012).
50. Whittingstall, K., Stroink, G. & Schmidt, M. Evaluating the spatial relationship of event-related potential and functional MRI sources in the primary visual cortex. *Hum Brain Mapp* **28**, 134-142, doi:10.1002/hbm.20265 (2007).
51. Elvsashagen, T. *et al.* The surface area of early visual cortex predicts the amplitude of the visual evoked potential. *Brain Struct Funct* **220**, 1229-1236, doi:10.1007/s00429-013-0703-7 (2015).
52. Fischl, B. FreeSurfer. *Neuroimage* **62**, 774-781, doi:https://doi.org/10.1016/j.neuroimage.2012.01.021 (2012).
53. Dale, A. M., Fischl, B. & Sereno, M. I. Cortical Surface-Based Analysis: I. Segmentation and Surface Reconstruction. *Neuroimage* **9**, 179-194, doi:https://doi.org/10.1006/nimg.1998.0395 (1999).
54. Fischl, B. *et al.* Automatically parcellating the human cerebral cortex. *Cereb Cortex* **14**, 11-22, doi:10.1093/cercor/bhg087 (2004).

55. Hinds, O. P. *et al.* Accurate prediction of V1 location from cortical folds in a surface coordinate system. *Neuroimage* **39**, 1585-1599, doi:10.1016/j.neuroimage.2007.10.033 (2008).
56. Rosen, A. F. G. *et al.* Quantitative assessment of structural image quality. *Neuroimage* **169**, 407-418, doi:10.1016/j.neuroimage.2017.12.059 (2018).
57. Normann, C., Schmitz, D., Furmaier, A., Doing, C. & Bach, M. Long-term plasticity of visually evoked potentials in humans is altered in major depression. *Biol Psychiatry* **62**, 373-380, doi:10.1016/j.biopsych.2006.10.006 (2007).
58. Valstad, M. *et al.* Experience-dependent modulation of the visual evoked potential: Testing effect sizes, retention over time, and associations with age in 415 healthy individuals. *Neuroimage* **223**, 117302, doi:10.1016/j.neuroimage.2020.117302 (2020).
59. Valstad, M. *et al.* Evidence for reduced long-term potentiation-like visual cortical plasticity in schizophrenia and bipolar disorder. *bioRxiv*, 2020.2006.2006.128926, doi:10.1101/2020.06.06.128926 (2020).
60. Delorme, A. & Makeig, S. EEGLAB: an open source toolbox for analysis of single-trial EEG dynamics including independent component analysis. *J Neurosci Methods* **134**, 9-21, doi:10.1016/j.jneumeth.2003.10.009 (2004).
61. Bigdely-Shamlo, N., Mullen, T., Kothe, C., Su, K. M. & Robbins, K. A. The PREP pipeline: standardized preprocessing for large-scale EEG analysis. *Front Neuroinform* **9**, 16, doi:10.3389/fninf.2015.00016 (2015).
62. Belouchrani, A., Abed-Meraim, K., Cardoso, J.-F. & Moulines, E. A blind source separation technique using second-order statistics. *IEEE Trans. Signal Process.* **45**, 434-444 (1997).
63. Chaumon, M., Bishop, D. V. & Busch, N. A. A practical guide to the selection of independent components of the electroencephalogram for artifact correction. *J Neurosci Methods* **250**, 47-63, doi:10.1016/j.jneumeth.2015.02.025 (2015).
64. Pajevic, S., Basser, P. J. & Fields, R. D. Role of myelin plasticity in oscillations and synchrony of neuronal activity. *Neuroscience* **276**, 135-147, doi:https://doi.org/10.1016/j.neuroscience.2013.11.007 (2014).
65. Dutta, D. J. *et al.* Regulation of myelin structure and conduction velocity by perinodal astrocytes. *Proceedings of the National Academy of Sciences* **115**, 11832-11837, doi:10.1073/pnas.1811013115 (2018).
66. Ishibashi, T. *et al.* Astrocytes promote myelination in response to electrical impulses. *Neuron* **49**, 823-832, doi:10.1016/j.neuron.2006.02.006 (2006).
67. Zalc, B. & Fields, R. D. Do Action Potentials Regulate Myelination? *Neuroscientist* **6**, 5-13, doi:10.1177/107385840000600109 (2000).
68. Dinse, J. *et al.* A cytoarchitecture-driven myelin model reveals area-specific signatures in human primary and secondary areas using ultra-high resolution in-vivo brain MRI. *Neuroimage* **114**, 71-87, doi:https://doi.org/10.1016/j.neuroimage.2015.04.023 (2015).

69. Peters, A. & Sethares, C. Myelinated axons and the pyramidal cell modules in monkey primary visual cortex. *J Comp Neurol* **365**, 232-255, doi:10.1002/(sici)1096-9861(19960205)365:2<232::Aid-cne3>3.0.Co;2-6 (1996).
70. Utzschneider, D. A. *et al.* Action potential conduction and sodium channel content in the optic nerve of the myelin-deficient rat. *Proc Biol Sci* **254**, 245-250, doi:10.1098/rspb.1993.0153 (1993).
71. Romanos, J., Benke, D., Saab, A. S., Zeilhofer, H. U. & Santello, M. Differences in glutamate uptake between cortical regions impact neuronal NMDA receptor activation. *Communications Biology* **2**, 127, doi:10.1038/s42003-019-0367-9 (2019).
72. Martin R. Gluck, M.D., Ph.D. „ Rohan G. Thomas, B.A. „ Kenneth L. Davis, M.D. , and & Vahram Haroutunian, Ph.D. Implications for Altered Glutamate and GABA Metabolism in the Dorsolateral Prefrontal Cortex of Aged Schizophrenic Patients. *American Journal of Psychiatry* **159**, 1165-1173, doi:10.1176/appi.ajp.159.7.1165 (2002).
73. Mavroudis, I. *et al.* Morphological alterations of the pyramidal and stellate cells of the visual cortex in schizophrenia. *Exp Ther Med* **22**, 669-669, doi:10.3892/etm.2021.10101 (2021).
74. Moyer, C. E., Shelton, M. A. & Sweet, R. A. Dendritic spine alterations in schizophrenia. *Neurosci Lett* **601**, 46-53, doi:10.1016/j.neulet.2014.11.042 (2015).
75. Faludi, G. & Mirnics, K. Synaptic changes in the brain of subjects with schizophrenia. *International Journal of Developmental Neuroscience* **29**, 305-309, doi:https://doi.org/10.1016/j.ijdevneu.2011.02.013 (2011).
76. Spencer, K. M. *et al.* Abnormal Neural Synchrony in Schizophrenia. *The Journal of Neuroscience* **23**, 7407, doi:10.1523/JNEUROSCI.23-19-07407.2003 (2003).
77. Uhlhaas, P. J. & Singer, W. Neural synchrony in brain disorders: relevance for cognitive dysfunctions and pathophysiology. *Neuron* **52**, 155-168, doi:10.1016/j.neuron.2006.09.020 (2006).
78. Ashok, A. H. *et al.* The dopamine hypothesis of bipolar affective disorder: the state of the art and implications for treatment. *Mol Psychiatry* **22**, 666-679, doi:10.1038/mp.2017.16 (2017).
79. Du, F. *et al.* Myelin and Axon Abnormalities in Schizophrenia Measured with Magnetic Resonance Imaging Techniques. *Biological Psychiatry* **74**, 451-457, doi:https://doi.org/10.1016/j.biopsych.2013.03.003 (2013).
80. Jorgensen, K. N. *et al.* Increased MRI-based cortical grey/white-matter contrast in sensory and motor regions in schizophrenia and bipolar disorder. *Psychol Med* **46**, 1971-1985, doi:10.1017/s0033291716000593 (2016).
81. Kelly, S. *et al.* Widespread white matter microstructural differences in schizophrenia across 4322 individuals: results from the ENIGMA Schizophrenia DTI Working Group. *Mol Psychiatry* **23**, 1261-1269, doi:10.1038/mp.2017.170 (2018).
82. Takahashi, N., Sakurai, T., Davis, K. L. & Buxbaum, J. D. Linking oligodendrocyte and myelin dysfunction to neurocircuitry abnormalities in schizophrenia. *Progress in Neurobiology* **93**, 13-24, doi:https://doi.org/10.1016/j.pneurobio.2010.09.004 (2011).

83. Uranova, N. A., Vikhreva, O. V., Rachmanova, V. I. & Orlovskaya, D. D. Ultrastructural alterations of myelinated fibers and oligodendrocytes in the prefrontal cortex in schizophrenia: a postmortem morphometric study. *Schizophr Res Treatment* **2011**, 325789-325789, doi:10.1155/2011/325789 (2011).
84. Konopaske, G. T., Lange, N., Coyle, J. T. & Benes, F. M. Prefrontal cortical dendritic spine pathology in schizophrenia and bipolar disorder. *JAMA Psychiatry* **71**, 1323-1331, doi:10.1001/jamapsychiatry.2014.1582 (2014).
85. Paolicelli, R. C. *et al.* Synaptic pruning by microglia is necessary for normal brain development. *Science* **333**, 1456-1458, doi:10.1126/science.1202529 (2011).
86. Sellgren, C. M. *et al.* Increased synapse elimination by microglia in schizophrenia patient-derived models of synaptic pruning. *Nat Neurosci* **22**, 374-385, doi:10.1038/s41593-018-0334-7 (2019).
87. Grasby, K. L. *et al.* The genetic architecture of the human cerebral cortex. *Science* **367**, doi:10.1126/science.aay6690 (2020).
88. Panizzon, M. S. *et al.* Distinct genetic influences on cortical surface area and cortical thickness. *Cerebral cortex (New York, N.Y. : 1991)* **19**, 2728-2735, doi:10.1093/cercor/bhp026 (2009).
89. Pontious, A., Kowalczyk, T., Englund, C. & Hevner, R. F. Role of intermediate progenitor cells in cerebral cortex development. *Dev Neurosci* **30**, 24-32, doi:10.1159/000109848 (2008).
90. Rakic, P. Specification of cerebral cortical areas. *Science* **241**, 170, doi:10.1126/science.3291116 (1988).
91. Rakic, P. A small step for the cell, a giant leap for mankind: a hypothesis of neocortical expansion during evolution. *Trends in Neurosciences* **18**, 383-388, doi:https://doi.org/10.1016/0166-2236(95)93934-P (1995).
92. Strike, L. T. *et al.* Genetic Complexity of Cortical Structure: Differences in Genetic and Environmental Factors Influencing Cortical Surface Area and Thickness. *Cereb Cortex* **29**, 952-962, doi:10.1093/cercor/bhy002 (2019).
93. Wierenga, L. M., Langen, M., Oranje, B. & Durston, S. Unique developmental trajectories of cortical thickness and surface area. *Neuroimage* **87**, 120-126, doi:https://doi.org/10.1016/j.neuroimage.2013.11.010 (2014).
94. Winkler, A. M. *et al.* Cortical thickness or grey matter volume? The importance of selecting the phenotype for imaging genetics studies. *Neuroimage* **53**, 1135-1146, doi:10.1016/j.neuroimage.2009.12.028 (2010).
95. Norbom, L. B. *et al.* New insights into the dynamic development of the cerebral cortex in childhood and adolescence: Integrating macro- and microstructural MRI findings. *Progress in Neurobiology*, 102109, doi:https://doi.org/10.1016/j.pneurobio.2021.102109 (2021).
96. Birnbaum, R. & Weinberger, D. R. Genetic insights into the neurodevelopmental origins of schizophrenia. *Nature Reviews Neuroscience* **18**, 727-740, doi:10.1038/nrn.2017.125 (2017).
97. Hyde, K. L. *et al.* Cortical Thickness in Congenital Amusia: When Less Is Better Than More. *The Journal of Neuroscience* **27**, 13028, doi:10.1523/JNEUROSCI.3039-07.2007 (2007).

98. Liem, F., Zaehle, T., Burkhard, A., Jancke, L. & Meyer, M. Cortical thickness of supratemporal plane predicts auditory N1 amplitude. *Neuroreport* **23**, 1026-1030, doi:10.1097/WNR.0b013e32835abc5c (2012).
99. Hogstrom, L. J., Westlye, L. T., Walhovd, K. B. & Fjell, A. M. The structure of the cerebral cortex across adult life: age-related patterns of surface area, thickness, and gyrification. *Cereb Cortex* **23**, 2521-2530, doi:10.1093/cercor/bhs231 (2013).

# Figures

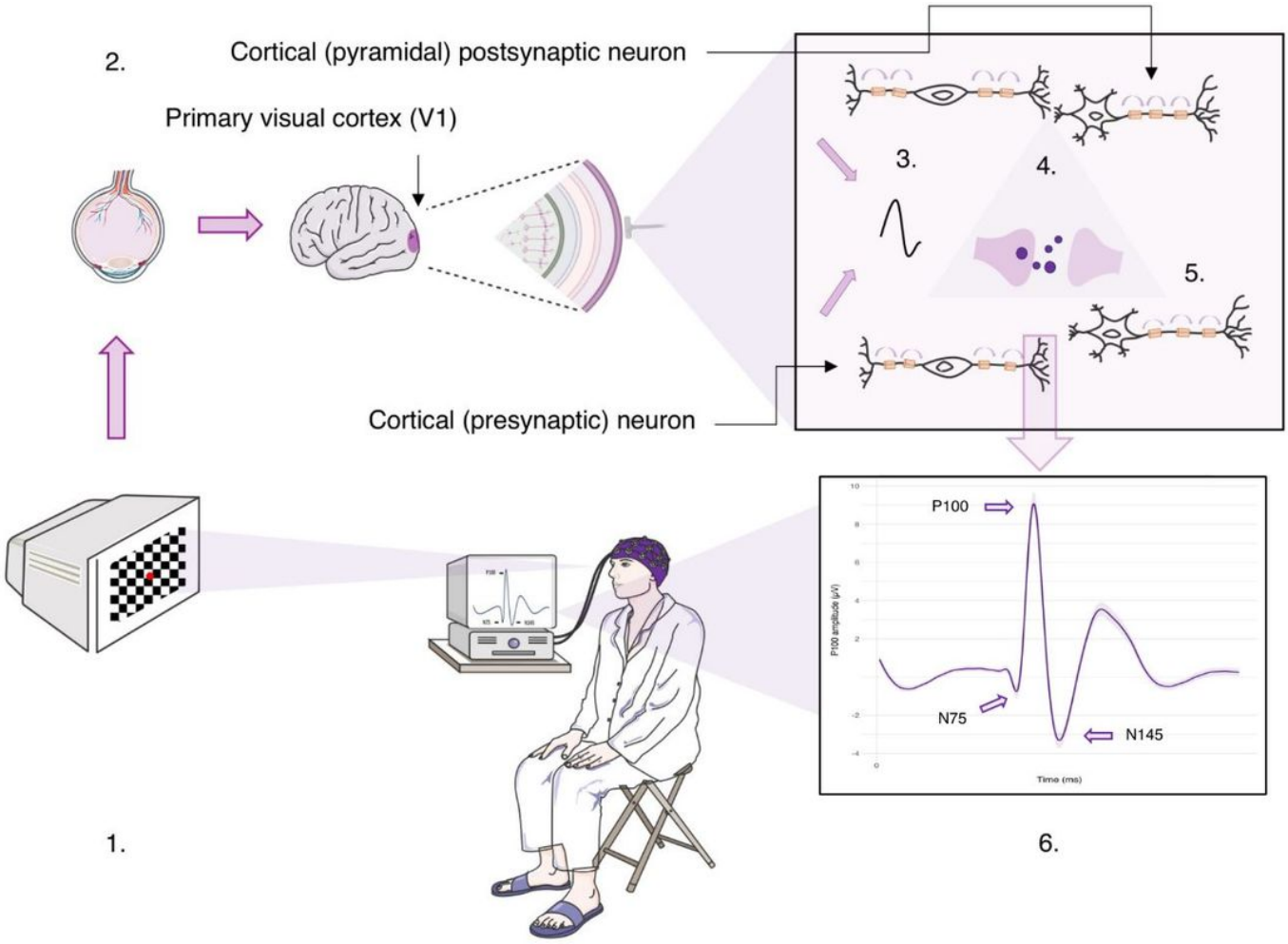


**Figure 1**

Visual Evoked Potential. The figure illustrates how visual stimuli in the form of checkerboard reversals stimulates the visual system all the way from the retina to the primary visual cortex (V1) and how the visual evoked potentials (VEPs) can be recorded with scalp-EEG. Step 1. Scalp-EEG is recorded while the participant is focusing on a red dot in the middle of a computer screen (placed approximately 50 cm in front of them) while exposed to reversals of checkerboards. Step 2. The reversal of checkerboards (white squares change color to black and vice versa) stimulates the visual system to send electrical impulses from the retina, through the optic nerve and towards V1. Step 3. When the electrical impulses reach V1,

presynaptic neurons (interneurons) generate action potentials (Aps) that trigger the presynaptic cells to release neurotransmitters from the presynaptic terminals into the synaptic clefts. Step 4. Binding of the neurotransmitters to receptors on the postsynaptic neurons (pyramidal cells) generate temporary changes in the postsynaptic membrane potentials, also known as postsynaptic potentials (PSPs). Step 5. Summation of PSPs from a large number of synchronized pyramidal neurons can be recorded from scalp electrodes overlying the V1 area. Step 6. Grand average VEPs measured at the occiput (Oz) with anterior reference (AFz) during intervention phase of the first VEP paradigm that lasted for 10 min, yielding a total of 1200 reversals. Ms=milliseconds; μV=microvolts. Parts of the symbols used in figure 1 are taken from Servier Medical Art (https://smart.servier.com/).

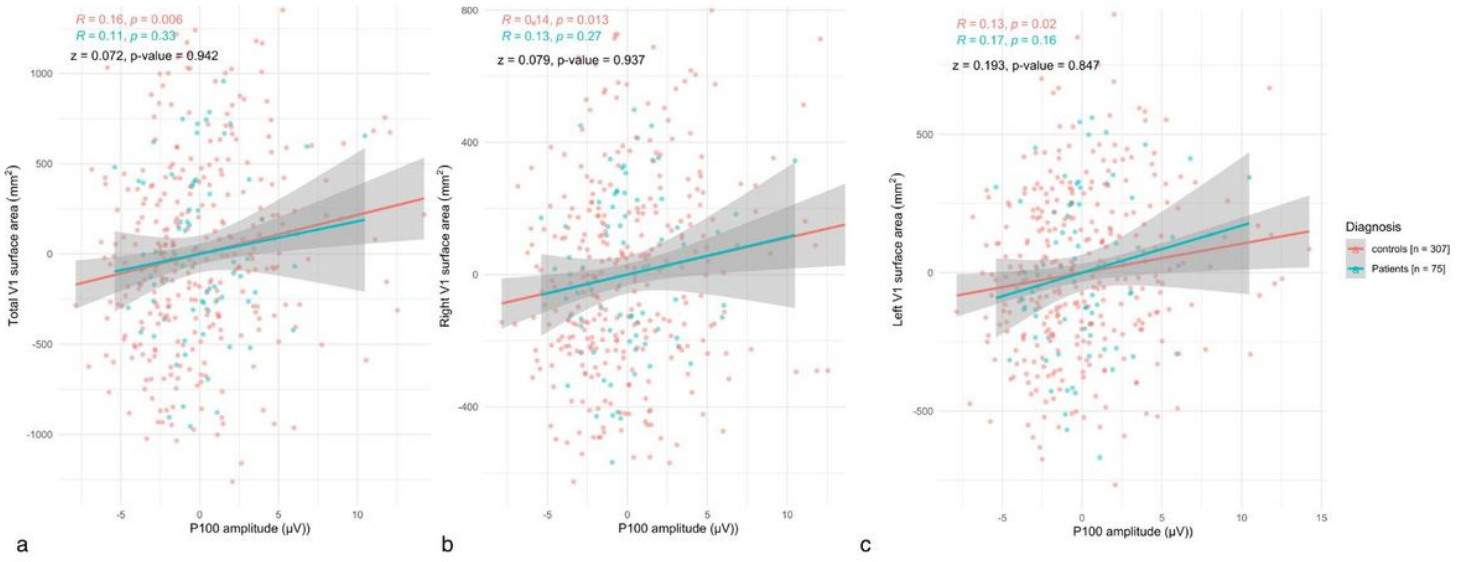


## Figure 2

a Pearson correlation between the P100 amplitude and total V1 surface area in healthy individuals and in patients. b Pearson correlation between the P100 amplitude and right V1 surface area in healthy individuals and in patients. c Pearson correlation between the P100 amplitude and left V1 surface area in healthy individuals and in patients. Results from the paired r test revealed a non- significant difference in the correlation between the P100 amplitude and the V1 surface area (total, right and left) between healthy individuals and patients (p>0.02).

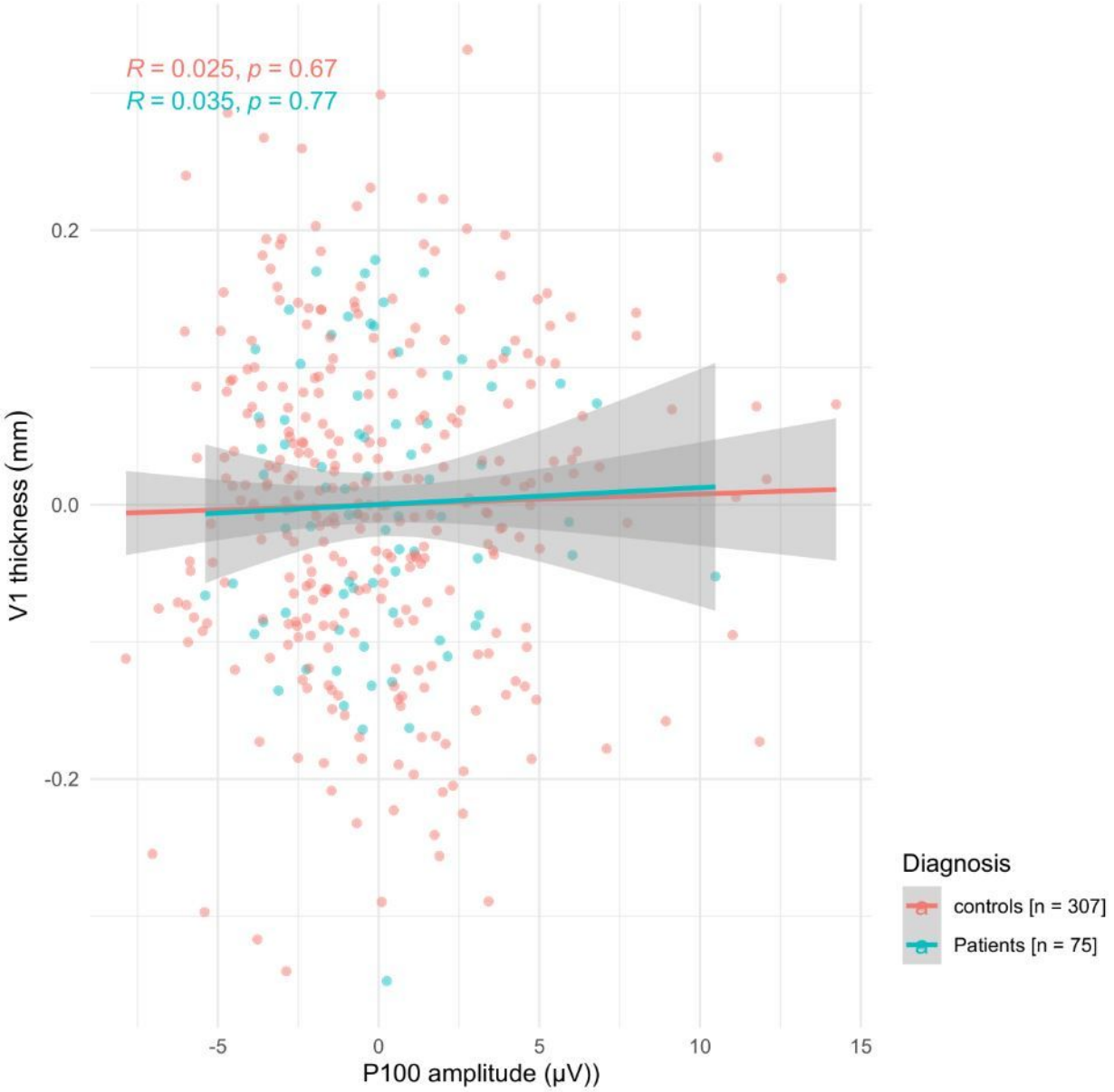


## Figure 3

Pearson correlation between P100 amplitude and the V1 cortical thickness in healthy individuals (n= 307) and patients (n=75) with SCZ spectrum and BD.

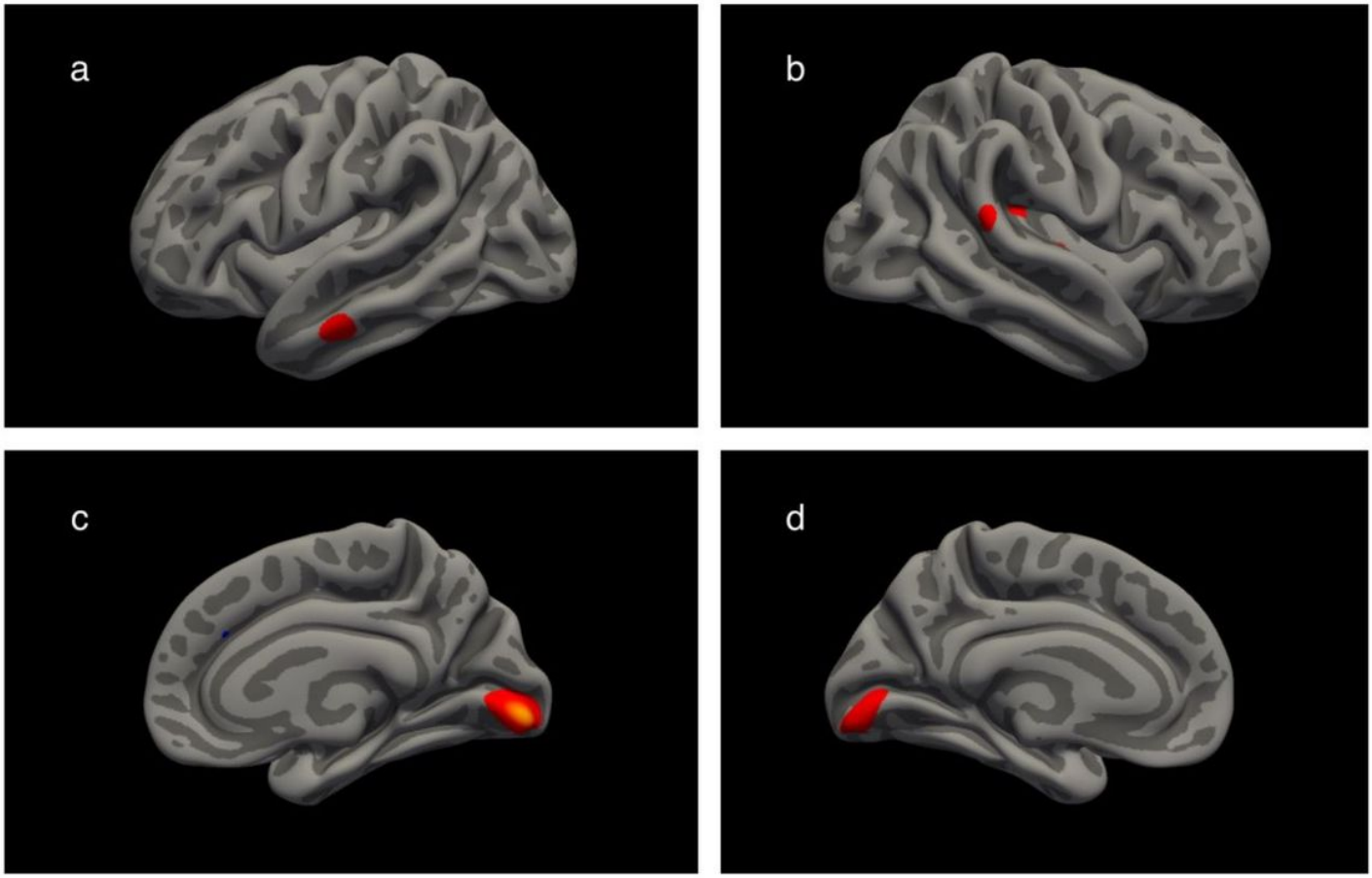


**Figure 4**

Vertex wise whole brain analyses testing the correlation between P100 amplitude and the surface area across the cortical mantle in the left and right hemispheres, in healthy individuals. Nominally significant correlations (threshold at an uncorrected alpha level of $p<0.01$) are displayed in red. a Lateral view of left hemisphere. b Lateral view of right hemisphere. c Medial view of the right hemisphere. d Medial view of the left hemisphere.

## Supplementary Files

This is a list of supplementary files associated with this preprint. Click to download.

- Supplementaryinformation.pdf
- FigS1.tiff
- FigS2.tiff
- FigS3.tiff
- FigS4.tiff
- FigS5.tiff

- FigS6.tiff
- FigS7.tiff